Published in final edited form as:
Curr Biol. 2012 August 21; 22(16): 1510–1515. doi:10.1016/j.cub.2012.05.055.

Exo70 Stimulates the Arp2/3 Complex-mediated Actin Branching for Lamellipodia Formation and Cell Migration

Jianglan Liu[1,4], **Yuting Zhao**[1,4], **Yujie Sun**[2], **Bing He**[1], **Changsong Yang**[1], **Tatyana Svitkina**[1,3], **Yale E. Goldman**[2,3], and **Wei Guo**[1,3,*]

[1]Department of Biology, University of Pennsylvania, Philadelphia, PA 19104, USA

[2]Department of Physiology and Biophysics, University of Pennsylvania, Philadelphia, PA 19104, USA

[3]Pennsylvania Muscle Institute, University of Pennsylvania, Philadelphia, PA 19104, USA

Summary

Directional cell migration requires the coordination of actin assembly and membrane remodeling. The exocyst is an octameric protein complex essential for exocytosis and plasma membrane remodeling [1,2]. A component of the exocyst, Exo70, directly interacts with the Arp2/3 complex, a core nucleating factor for the generation of branched actin networks for cell morphogenesis and migration [3-9]. Using *in vitro* actin polymerization assay and time-lapse TIRF microscopy, we found Exo70 functions as a kinetic activator of the Arp2/3 complex that promotes actin filament nucleation and branching. We further found that the effect of Exo70 on actin is mediated by promoting the interaction of Arp2/3 complex with WAVE2, a member of the N-WASP/WAVE family of nucleation promoting factors (NPFs). At the cellular level, the stimulatory effect of Exo70 on Arp2/3 is required for lamellipodia formation and maintaining directional persistence of cell migration. Our findings provide a novel mechanism for regulating actin polymerization and branching for effective membrane protrusion during cell morphogenesis and migration.

Results and Discussion

We have previously shown that Exo70 directly interacts with the Arp2/3 complex [7]. However, the molecular consequence and functional implication of this interaction is unknown. Here, we purified Exo70 and the Arp2/3 complex (Figure S1A, B) and performed polymerization assays using pyrene-labeled actin. Since the WAVE complexes are usually inactive [10], we used the recombinant WAVE2 as the nucleation-promoting factor in our assay. Exo70 alone or together with the Arp2/3 complex did not affect F-actin assembly. WAVE2 stimulated the Arp2/3 complex; further addition of Exo70 significantly enhanced actin polymerization (Figure 1A). The concentration of barbed ends in our experiment

[*]Correspondence: guowei@sas.upenn.edu.
[4]These authors contributed equally to this work.

Author Contributions: J.L., Y.Z. and W.G. conceived the project and designed experiments; J.L., Y.Z., C.Y., B.H. and Y.S. designed and/or carried out some of the experiments; J.L., Y.Z. and W.G. analyzed the data and wrote the manuscript. J.L. and Y.Z. contributed equally to this work.

Competing financial interests: The authors declare no competing financial interests.

setting (2μM G-actin, 25 nM WAVE2, and 15 nM Arp2/3) was 0.22 nM in the absence of Exo70, and was 0.41 nM in the presence of Exo70. The stimulatory effect of Exo70 is dose-dependent (Figure 1B). Furthermore, in the presence of saturating concentration of Exo70 (1 μM), significantly less WAVE2 is required (reduced from 25 nM to 6.25 nM) for Arp2/3 activation (Figure S1C).

We have previously found that Exo70 lacking residues 628-630 had a weaker interaction with the Arp2/3 complex [7]. Indeed, Exo70(Δ628–630) had a much lower stimulatory effect on actin polymerization than the wild type Exo70 (Figure 1A). Addition of Exo70 reduced the time to reach half maximal polymerization by 2.4-fold, whereas Exo70(Δ628–630) had a much weaker effect (Figure 1C). The maximal rate of actin polymerization was increased by 100% with Exo70, but only 34% with Exo70(Δ628–630) (Figure 1D).

Upon activation by WAVE2, the Arp2/3 complex generates new actin branches on the side of pre-existing actin filaments, which can be monitored by total internal reflection fluorescence microscopy (TIRFM) [11]. Here we examined the effect of Exo70 on actin branching in real-time using TIRFM. To better visualize branching and elongation of the new filaments, we performed dual-color imaging to better differentiate the pre-existing and newly formed actin filaments. Rhodamine-labeled G-actin was allowed to polymerize for 3 mins and captured onto the surface of a coverslip coated with NEM-myosin. Then Cy5-labeled G-actin together with Arp2/3, WAVE2, wild type or mutant Exo70 was flown into the chamber to replace Rhodamine-labeled G-actin. The newly generated actin filaments were monitored over time. In the presence of Arp2/3 and WAVE2, branches were generated from the sides of actin filaments (Figure 2A, upper panel; see Movie S1 for both audio and visual presentation of the generation of new branches; see Figure S2 for enlarged images). Addition of Exo70 significantly stimulated branch formation (Figure 2A, middle panel; Movie S2 and Figure S2). The Exo70(Δ628–630) mutant barely had any stimulatory effect (Figure 2A, bottom panel; Movie S3). Addition of Exo70 in the absence of WAVE2 had no effect on actin (Movie S4). After 240 seconds, the branching ratio (number of branches/number of total actin filaments) was 6-fold higher in the presence of Exo70 (Figure 2B). The lengths of the newly generated actin filaments were also measured. In reactions with Exo70, the actin filaments were slightly shorter than those without Exo70 (Figure 2C), suggesting that, when the total amount of G-actin is limited (0.8 μM of 8% Cy5-labeled G-actin, in contrast to 2 μM G-actin in the pyrene actin assay), an increase in actin branching results in a reduction of the final length of the filaments.

Since the effect of Exo70 is shown only in the presence of WAVE2, Exo70 itself is unlikely to be an actin nucleator or a nucleation-promoting factor (NPF). Then what is the molecular mechanism by which Exo70 stimulates the Arp2/3 complex? Exo70 binds to the Arp2/3 complex through its ARPC1 subunit (a.k.a. p40 or Arc40), which physically contacts N-WASP/WAVE [12-14]. It is thus possible that Exo70 affects the WAVE2-Arp2/3 interaction, which in turn promotes the Arp2/3 complex activation. To test this possibility, we first performed *in vitro* binding assay using GST-WAVE2 and purified Arp2/3 complex (Figure 3A). In the presence of Exo70, the amount of Arp2/3 bound to GST-WAVE2 increased by 3.5-fold (Figure 3B). As a negative control, GST-Rabin8, a fusion protein with a similar molecular weight to Exo70, did not bind to the Arp2/3 complex. The affinity of the Arp2/3 complex to WAVE2 is much higher in the presence of Exo70 (kd=210 nM) than without Exo70 (kd=470 nM) (Figure S3A). To examine whether Exo70 affects the WAVE2-Arp2/3 interaction in cells, immunoprecipitation experiments were carried out using cells expressing FLAG-WAVE2 (Figure 3C). When Exo70 was knocked down by siRNA, only 44% of Arp3 was co-precipitated with WAVE2 comparing with control siRNA-treated cells (Figure 3D). Reciprocally, when ARPC1 was knocked down by siRNA, endogenous Exo70 was no longer co-precipitated with WAVE2 (Figure 3E). Consistent with the finding, the

Exo70(Δ628–630) mutant interacts much weakly with WAVE2 in comparison to the wild type Exo70 as tested by co-immunoprecipitation experiments (Figure 3F) and pull down experiments (Figure S3B). Taken together, our data strongly suggested that Exo70 positively regulates the interaction between the Arp2/3 complex and WAVE2, and provide a molecular basis for our observed stimulatory effect of Exo70 on Arp2/3 activation.

To examine the physiological function of Exo70 in the stimulation of the Arp2/3 complex, we generated human MDA-MB-231 stable cell lines expressing GFP-tagged rat wild type Exo70 and a Exo70(Δ628-630) mutant that is defective in stimulating the Arp2/3 complex (see above). The endogenous Exo70 was then knocked down by siRNA in these cells (Figure S4A). The levels of other exocyst subunits, WAVE2 and Arp3 were not affected in the knockdown cells (Figure S4B), and Exo70(Δ628-630) binds to Sec8 to the same extent as the wild type (Figure S4C). As shown in Figure 4A, the Exo70-knockdown cells expressing Exo70(Δ628-630) failed to form lamellipodia as indicated by Arp3 and F-actin staining. The “lamellipodia ratio”, defined as the lamellipodia length divided by the total cell perimeter, was significantly lower in the knockdown cells expressing Exo70(Δ628-630) (Figure 4B). The migratory properties of these cells were also examined. In transwell assays, the number of mutant Exo70 cells migrated to the lower chamber was much smaller than the control cells (Figure 4C). Also, using a wound-healing assay, we found that Exo70 siRNA knockdown cells expressing Exo70(Δ628-630) took more time for wound closure (Figure 4D and Figure S4D). By tracking the trajectories of individual cells over time, we found that cells expressing Exo70(Δ628-630) were not only slower in migration, but also less capable of maintaining the direction of their movement (Figure 4E, F). The directional persistence, quantified as the ratio of net displacement to the total migration distance (“D:T ratio”), was much smaller in cells expressing Exo70(Δ628-630) (Figure 4E). These results suggest that the function of Exo70 in stimulating the Arp2/3 complex plays an important role in membrane protrusion formation and directional cell migration.

Our experiments, for the first time, revealed that Exo70 is able to kinetically stimulate the Arp2/3 complex in the presence of WAVE2 for actin polymerization and branching. Exo70 binds to the Arp2/3 complex through ARPC1, the subunit that physically contacts N-WASP/WAVE for activation [12-14]. Our data show that Exo70 stimulates the interaction between the Arp2/3 complex and WAVE2, which may provide a molecular mechanism for the observed stimulatory effect of Exo70 on the Arp2/3 complex activation. During membrane protrusion formation, associated with actin assembly is dynamic membrane reorganization [15,16]. Exo70, as a member of the exocyst complex, is involved in post-Golgi exocytosis and membrane remodeling ([17]; Guo lab unpublished data). The effect of Exo70 on Arp2/3-mediated actin polymerization and branching may couple actin dynamics and membrane reorganization for cell morphogenesis and effective migration.

We have previously shown that the Exo70-Arp2/3 complex interaction is stronger in cells treated with EGF [7], or expressing Y527F c-Src [18], which are known to stimulate membrane protrusion and cell migration. These observations suggest that, in cells, the effect of Exo70 on the Arp2/3 complex is up-regulated by signaling events to levels above what we observed here using recombinant proteins. It is possible that the activation of Exo70 and/or the Arp2/3 complex by small GTP-binding proteins or kinases in response to growth factors stimulates their interaction. Future investigation of this regulation will lead to better understanding of many processes such as chemotaxis and tumor cell invasion.

Experimental Procedures

Detailed information on plasmids, antibodies, cell culture, protein purification, immunoprecipitation and *in vitro* binding assay, fluorescence microscopy, wound-healing

assay, transwell assay, individual cell movement tracking is described in the Supplemental Experimental Procedures.

Pyrene actin assay

Pyrene actin polymerization assay was performed as previously described [19, 20]. The kinetics of actin polymerization was monitored by pyrene fluorescence with excitation at 370 nm and emission at 410 nm. Proteins to be tested for each reaction (15 nM Arp2/3, 25 nM WAVE2, 1 μM of GST, wild type or mutant Exo70 were mixed and diluted in 90 μl polymerization buffer (60 mM KC1, 2.5 mM NaCl, 0.6 mM $MgCl_2$, 5 mM Tris-HCl, pH 7.5, 2.5 mM HEPES, pH 7.1, 0.5 mM EGTA, 30 μM $CaCl_2$, 0.2 mM ATP, and 0.3 mM NaN_3), then pre-incubated for 30 mins at 4°C prior to the addition to the actin assembly mix. 20% pyrenyl-labeled actin was prepared using pyrene-labeled muscle actin and unlabeled muscle actin (Cytoskeleton Inc.). 11.5 μl G-actin (20.9 μM, 20% pyrenyl-labeled) in G-actin buffer (Triethylamine, 0.3mM $CaCl_2$, 0.1mM EDTA, 0.7mM ATP, 6.25mM NaN_3) was converted to Mg-G-actin by mixing with 18.5 μl Mg^{2+} converting buffer (1.6 mM Tris-HCl, pH8, 0.18 mM EGTA, and 0.51 mM $MgCl_2$) for 5 min. The converted actin mixture was then diluted into 90μl protein mixture with a final G-actin concentration of 2 μM, and immediately transferred into a cuvette and monitored for the increase in fluorescence at 410 nm in a fluorescence spectrophotometer. Polymerization kinetics was anlyzed using Excel (Microsoft). The polymerization rate was represented as the maximal slope of the elongation phase of each curve. Statistical analyses were performed using the paired Student's *t*-test (n=3). Measurement of barbed ends is performed as previously described [21].

Visualization of actin polymerization in real time by TIRFM

TIRF-based actin branching assay was performed as previously described [11] with modifications. Total internal reflection excitation was generated on a Nikon TE2000U inverted microscope with an in-house TIRF illuminator using objective-type (Nikon 100×, Plan-achromat 1.49 NA oil immersion objective) TIRF excitation. Images were collected using a back-illuminated electron multiplying-CCD camera (Cascade-512B, Photometrics). Two-color ALEX (Alternating-laser excitation) [22] was used for fluorescence excitation. A solid-state 532-nm laser (CrystaLaser) and a Helium-Neon red laser (NEC, 10mW max) were used for excitation of Rhodamine-actin and Cy5-actin, respectively. Frame rate was set at 0.5 frame per second. To minimize photo-bleaching, laser intensities were reduced either by a neutral density filter or an intensity attenuator comprising a half-wave plate and a polarizer. Exposure time was set at ~ 400 ms and laser framing were synchronized with the camera shutter through a pulse sent from the camera.

Experiments were carried out in flow chambers assembled by mounting a pre-cleaned coverslip to a standard glass slide using Dow Corning 732 multi-purpose silicone sealant as spacers. Before use, the flow chambers were coated with NEM-myosin by flowing in 50 nM NEM-myosin in high salt buffer (500 mM KC1) and incubating for 1.5 min. The flow chambers were then treated with 1% BSA for 4 min to prevent non-specific binding to the surface. 15 nM Arp2/3, 25 nM WAVE2, 250 nM wild type or mutant Exo70 were mixed in the actin polymerization buffer and incubated at 4°C for 30 mins. 2 μM 6% Rhodamine-labeled actin was first converted to Mg-G-actin, and added to the flow chamber for polymerization. Rhodamine-labeled actin polymerization was allowed to proceed for 3 mins. Then a polymerization buffer containing 0.8 μM 8% Cy5-labeled Mg-G-actin together with 15 nM Arp2/3 complex, 25 nM WAVE2, 250 nM wild type or mutant Exo70 were added into the chamber to replace Rhodamine-labeled actin in the solution. Images were collected immediately after the addition of Cy5-labeled actin. For each ALEX cycle, Cy5 actin was imaged for 9 frames and Rhodamine actin 2 frames. Images were recorded for 10 min after the polymerization started. Average lengths of newly formed Cy5-actin filaments were

measured over time from 25 individual actin filaments for samples with or without Exo70 using ImageJ 1.73v software (http://rsb.info.nih.gov/ij/). Statistical analyses were performed using Student's *t*-test.

Supplementary Material

Refer to Web version on PubMed Central for supplementary material.

Acknowledgments

We thank Drs. Sally Zigmond, Bruce Goode, Shu-Chan Hsu, Shanshan Feng, Peng Yue, Michael Rosen, Henry Higgs, Giorgio Scita, Jeffery Peterson, and Roberto Dominguez for reagents and helpful discussions. The research is supported by National Institutes of Health grants (GM085146) to W.G. and T.S. Y.Z. is supported by an American Heart Association pre-doctoral fellowship. The JEOL 1011 transmission electron microscope was supported by the NIH Shared Instrumentation Grant to T.S.

References

1. Munson M, Novick P. The exocyst defrocked, a framework of rods revealed. Nat Struct Mol Biol. 2006; 13:577–581. [PubMed: 16826234]
2. He B, Guo W. The exocyst complex in polarized exocytosis. Curr Opin Cell Biol. 2009; 21:537–542. [PubMed: 19473826]
3. Pollard TD, Borisy GG. Cellular motility driven by assembly and disassembly of actin filaments. Cell. 2003; 112:453–465. [PubMed: 12600310]
4. Goley ED, Welch MD. The ARP2/3 complex: an actin nucleator comes of age. Nat Rev Mol Cell Biol. 2006; 7:713–726. [PubMed: 16990851]
5. Welch MD, Mullins RD. Cellular control of actin nucleation. Annu Rev Cell Dev Biol. 2002; 18:247–88. [PubMed: 12142287]
6. Ridley AJ. Life at the leading edge. Cell. 2011; 145:1012–1022. [PubMed: 21703446]
7. Zuo X, Zhang J, Zhang Y, Hsu SC, Zhou D, Guo W. Exo70 interacts with the Arp2/3 complex and regulates cell migration. Nat Cell Biol. 2006; 8:1383–1388. [PubMed: 17086175]
8. Insall RH, Machesky LM. Actin dynamics at the leading edge: from simple machinery to complex networks. Dev Cell. 2009; 17:310–22. [PubMed: 19758556]
9. Le Clainche C, Carlier MF. Regulation of actin assembly associated with protrusion and adhesion in cell migration. Physiol Rev. 2008; 88:489–513. [PubMed: 18391171]
10. Lebensohn AM, Kirschner MW. Activation of the WAVE complex by coincident signals controls actin assembly. Mol Cell. 2009; 36:512–524. [PubMed: 19917258]
11. Amann KJ, Pollard TD. Direct real-time observation of actin filament branching mediated by Arp2/3 complex using total internal reflection fluorescence microscopy. Proc Natl Acad Sci USA. 2001; 98:15009–15013. [PubMed: 11742068]
12. Pan F, Egile C, Lipkin T, Li R. ARPC1/Arc40 mediates the interaction of the actin-related protein 2 and 3 complex with Wiskott-Aldrich syndrome protein family activators. J Biol Chem. 2004; 279:54629–54636. [PubMed: 15485833]
13. Kelly AE, Kranitz H, Dotsch V, Mullins RD. Actin binding to the central domain of WASP/Scar proteins plays a critical role in the activation of the Arp2/3 complex. J Biol Chem. 2006; 281:10589–10597. [PubMed: 16403731]
14. Balcer HI, Daugherty-Clarke K, Goode BL. The p40/ARPC1 subunit of Arp2/3 complex performs multiple essential roles in WASp-regulated actin nucleation. J Biol Chem. 2010; 285:8481–8491. [PubMed: 20071330]
15. Scita G, Confalonieri S, Lappalainen P, Suetsugu S. IRSp53: crossing the road of membrane and actin dynamics in the formation of membrane protrusions. Trends Cell Biol. 2008; 18:52–60. [PubMed: 18215522]
16. Zhao H, Pykalainen A, Lappalainen P. I-BAR domain proteins: linking actin and plasma membrane dynamics. Curr Opin Cell Biol. 2011; 23:14–21. [PubMed: 21093245]

17. Liu J, Zuo X, Yue P, Guo W. Phosphatidylinositol 4,5-bisphosphate mediates the targeting of the exocyst to the plasma membrane for exocytosis in mammalian cells. Mol Biol Cell. 2007; 18:4483–4492. [PubMed: 17761530]

18. Liu J, Yue P, Artym VV, Mueller SC, Guo W. The role of the exocyst in matrix metalloproteinase secretion and actin dynamics during tumor cell invadopodia formation. Mol Biol Cell. 2009; 20:3763–3771. [PubMed: 19535457]

19. Kouyama T, Mihashi K. Fluorimetry study of N-(1-pyrenyl)iodoacetamide-labelled F-actin. Local structural change of actin protomer both on polymerization and on binding of heavy meromyosin. Eur J Biochem. 1981; 114:33–38. [PubMed: 7011802]

20. Zigmond S. In vitro actin polymerization using polymorphonuclear leukocyte extracts. Methods Enzymol. 2000; 325:237–254. [PubMed: 11036607]

21. Higgs HN, Blanchoin L, Pollard TD. Influence of the C terminus of Wiskott-Aldrich syndrome protein (WASp) and the Arp2/3 complex on actin polymerization. Biochemistry. 1999; 38:15212–15222. [PubMed: 10563804]

22. Kapanidis AN, Laurence TA, Lee NK, Margeat E, Kong X, Weiss S. Alternating-laser excitation of single molecules. Acc Chem Res. 2005; 38:523–533. [PubMed: 16028886]

Highlights

- Exo70 kinetically stimulates the Arp2/3 complex-mediated actin assembly
- The Exo70-ARPC1 interaction is required for stimulating the Arp2/3 complex
- Exo70 promotes the interaction between the Arp2/3 complex and WAVE2
- The Exo70-Arp2/3 interaction regulates lamellipodia formation and cell migration

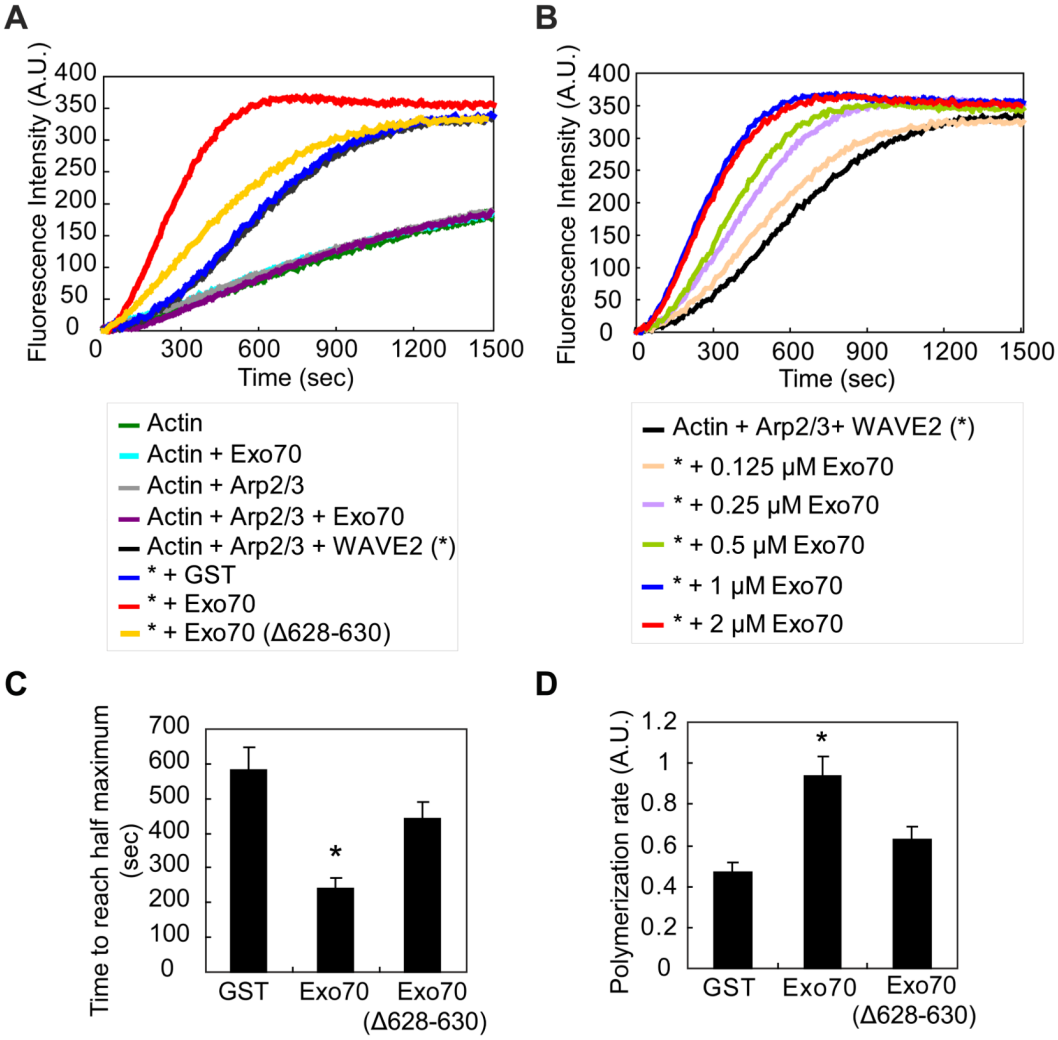

Figure 1. Exo70 stimulates Arp2/3-mediated actin polymerization

(A) The effect of Exo70 on Arp2/3-mediated actin polymerization was examined using the pyrene actin assay (2 μM of 20% pyrenyl-labeled G-actin, 15 nM Arp2/3, 25 nM WAVE2, 1 μM of GST, Exo70 or Exo70(Δ628-630). WAVE2 enhanced Arp/3-mediated actin polymerization (black). The addition of Exo70 further promoted actin assembly (red). In the absence of WAVE2, Exo70 has no effect on actin polymerization (light blue and dark purple). As a control, GST had no effect on the kinetics of actin polymerization mediated by Arp2/3 and WAVE2 (blue). The Exo70(Δ628-630) mutant defective in binding Arp2/3 has a much reduced stimulatory effect (yellow). A.U., arbitrary units. **(B)** Exo70 stimulates Arp2/3-mediated actin polymerization in a dose-dependent manner. The graph shows the effects of 0 to 2μM Exo70 on Arp2/3-mediated actin polymerization in the presence of WAVE2. **(C)** Time to reach half maximal actin polymerization, and **(D)** the rate of actin polymerization during the elongation phase was compared among different treatments. The polymerization rates were represented as the maximal slope of the elongation phase of each curve. A.U., arbitrary units. Error bars represent standard deviation. n=3. *, $p < 0.01$.

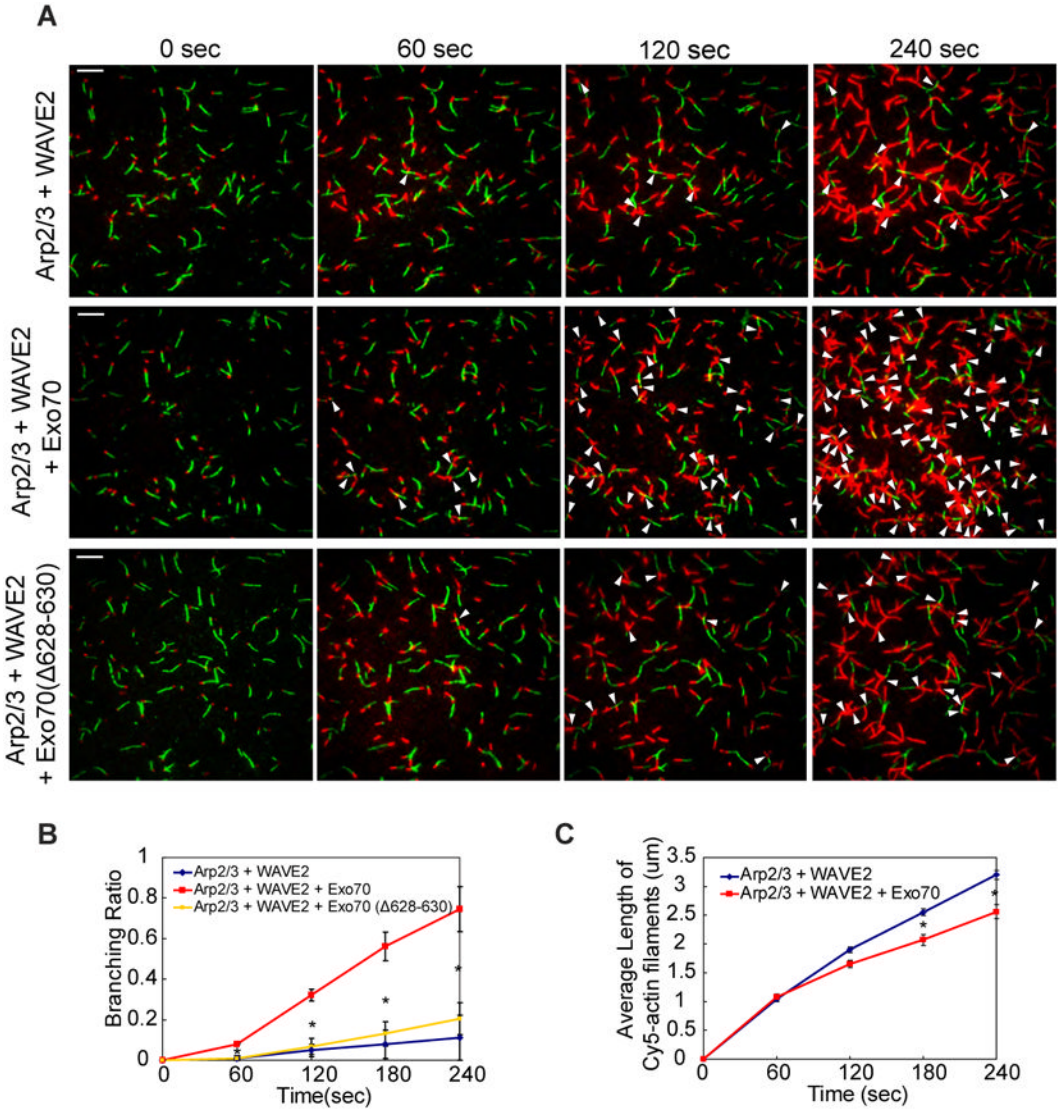

Figure 2. Exo70 stimulates the branching activity of the Arp2/3 complex in the presence of WAVE2

(A) Actin branching and elongation were monitored in real time using dual-color time-lapse TIRFM. 2 μM of 6% Rhodamine-labeled G-actin was allowed to polymerize. The resulting actin filaments (shown in green) were captured on the surface of a flow chamber pre-coated with NEM-myosin. After 3 mins, 0.8 μM of 8% Cy5-labeled actin (shown in red) together with 15 nM Arp2/3, 25 nM WAVE2, 250 nM Exo70 or Exo70(Δ628-630) were flowed in to replace Rhodamine-labeled G-actin. The newly generated actin filaments (marked in red) were monitored over time. Frames shown were collected at 0, 60, 120, and 240 sec after addition of the Cy5-G-actin and protein mixture. The white arrows indicate the positions where new actin filaments were generated from existing filament (the branching points). See Movies S1-S4 for better visual and audio presentations of the emergence of actin branches over time. Addition of Exo70 stimulated the generation of new branches (middle panel). The stimulatory effect was barely detectable with the Exo70(Δ628-630) mutant protein (lower panel). Scale bar, 5 μm. **(B)** Quantification of branching over time. Branching ratio is defined as the branch numbers divided by the numbers of total actin filaments in an illuminated field. Error bars represents standard deviation. n=3. $p < 0.01$ for samples with

wild type Exo70 over those with no Exo70 or the Exo70(Δ628-630) mutant at 120 sec, 180 sec, and 240 sec. Scale bar, 5 μm. **(C)** Average lengths of actin filaments over time for samples with or without Exo70. Error bars, standard deviation. n=25. $p < 0.01$ for samples with wild type Exo70 over those without Exo70 at 180 sec and 240 sec.

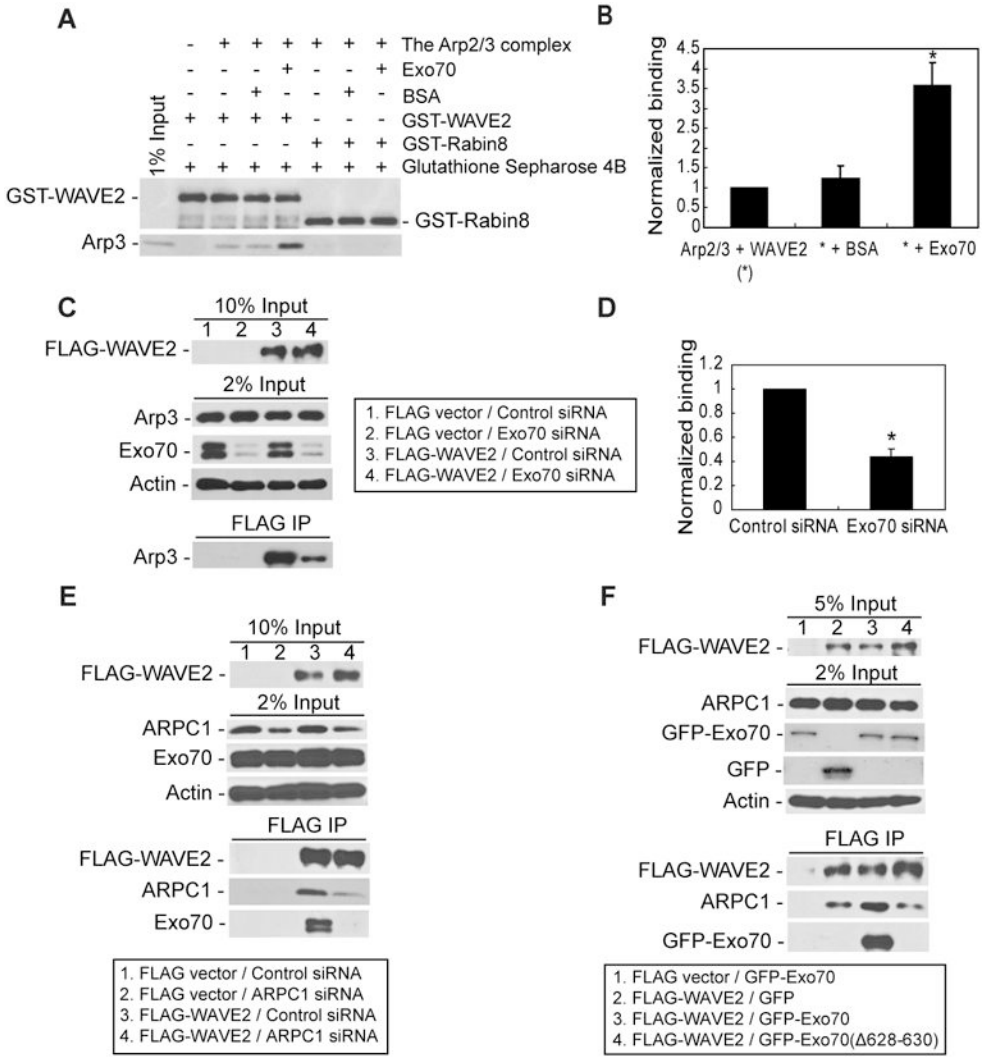

Figure 3. Exo70 promotes the interaction between the Arp2/3 complex and WAVE2

(A) 10 nM of the Arp2/3 complex was incubated with GST-WAVE2 or GST-Rabin8 conjugated to glutathione Sepharose 4B in the presence of 500 nM Exo70 or BSA. The input and bound proteins were analyzed by Western blots using anti-GST (upper panel) and anti-Arp3 antibodies (lower panel). **(B)** Quantification of the bound Arp3. Addition of Exo70 led to a 3.5-fold increase in GST-WAVE2-Arp3 binding. Error bars, SD. n=3; *, $p<0.01$. **(C)** Lysates of MDA-MB-231 cells expressing FLAG vector (lane 1 & 2) or FLAG-WAVE2 (lane 3 & 4) treated with control siRNA (lane 1 & 3) or Exo70 siRNA (lane 2 & 4) were incubated with anti-FLAG beads. The inputs and bound proteins were analyzed by western blots. **(D)** Quantification of Arp3 bound to FLAG-WAVE2. Knockdown of Exo70 led to a decrease of the binding of Arp3 to FLAG-WAVE2 to 44% of the control level. Error bars, SD. n=3; *, $p<0.01$. **(E)** RNAi knockdown of ARPC1 blocks the Exo70-WAVE2 interaction. Lysates of MDA-MB-231 cells expressing FLAG vector (lane 1 & 2) or FLAG-WAVE2 (lane 3 & 4) treated with Luciferase siRNA (lane 1 & 3) or ARPC1 siRNA (lane 2 & 4) were incubated with anti-FLAG antibody Sepharose. The inputs and bound proteins (FLAG-WAVE2, Arp3, and Exo70) were analyzed by western blots. **(F)** The Exo70(Δ628-630) mutant failed to co-immunoprecipitate with WAVE2. Lysates from MDA-MB-231 cells expressing FLAG vector (lane 1) or FLAG-WAVE2 (lane 2-4) with

GFP-Exo70 variants or GFP alone were incubated with the anti-FLAG Sepharose. The inputs and bound proteins were analyzed by western blots.

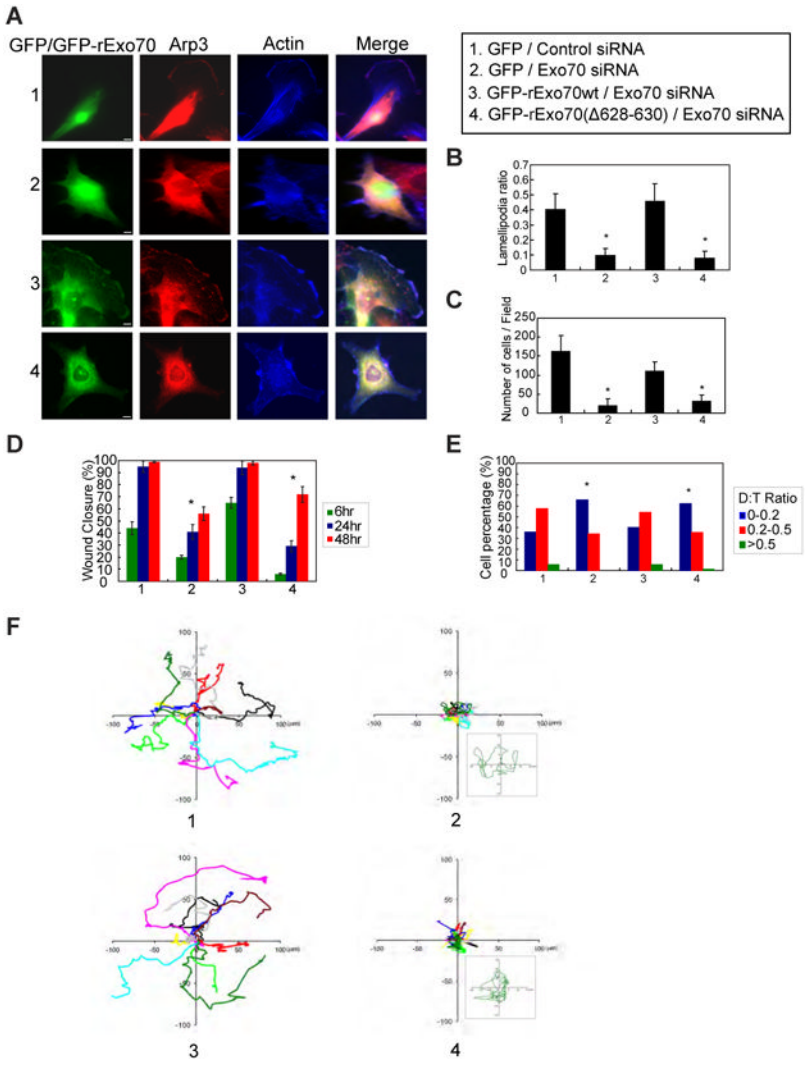

Figure 4. The function of Exo70 in Arp2/3 stimulation is required for lamellipodia formation and directional cell migration

(A) Cells expressing GFP-tagged rat wild type Exo70 or the Exo70(Δ628-630) mutant were stained for Arp3 (red) and F-actin (blue) to detect lamellipodia. Control siRNA-treated cells (Panel 1) had clear and extended lamellipodia. In Exo70-knockdown cells (Panel 2), the formation of lamellipodia was impaired. Expression of GFP-rExo70 (Panel 3) rescued lamellipodia formation, whereas the expression of Exo70(Δ628-630) failed to rescue the defect (Panel 4). Scale bar, 5 μm. **(B)** The ratios between the length of the lamellipodia and the total cell perimeters ("lamellipodium ratio") were compared for each group. The mutant group has lower lamellipodium ratios. Error bars, SD. n=25; *, $p<0.01$. (C) Transwell assay was performed using these cells. The bars indicate the average number of migrated cells per field for each group. n=3. *, $p<0.01$. **(D)** Wound-healing assays were performed using cells described above. The percentage of wound closure (closure distance/initial opening) after 6, 24, and 24 hrs of migration was calculated for each group. n=3. *, $p<0.01$. Also see Figure S4D for wound healing images. **(E)** Single cell movement was tracked using time-lapse microscopy. Directional persistence of individual cells was calculated as D:T ratio (see RESULTS). The percentage of cells with different D:T ratios (0-0.2; 0.2-0.5; >0.5) is indicated. n=60. *, $p<0.01$. **(F)** For each group, the trajectories of 10 representative cells at 5 min intervals during a 400-min migration period are presented. The origins of each track

were superimposed at position (0, 0). The boxed regions in corresponding treatments showed 7× magnified migration track from one representative cell in each group, which indicates that the cells were not stationary.